Journal of Photochemistry and Photobiology B: Biology 100 (2010) 1–9

Contents lists available at ScienceDirect

Journal of Photochemistry and Photobiology B: Biology

journal homepage: www.elsevier.com/locate/jphotobiol

One pot synthesis of new hybrid versatile nanocarrier exhibiting efficient stability in biological environment for use in photodynamic therapy

Edouard Thienot [a], Matthieu Germain [a], Kelthoum Piejos [a], Virginie Simon [a], Audrey Darmon [a], Julie Marill [a], Elsa Borghi [a], Laurent Levy [a], Jean-François Hochepied [b], Agnès Pottier [a,*]

[a] Nanobiotix SA, 60, Rue de Wattignies, F-75012 Paris, France
[b] Mines ParisTech, CEP/SCPI, 60, boulevard Saint-Michel, 75006 Paris, France

ARTICLE INFO

Article history:
Received 18 June 2009
Received in revised form 11 March 2010
Accepted 22 March 2010
Available online 30 March 2010

Keywords:
Nanotechnology
Hybrid nanocarrier
Photodynamic therapy
Cancer

ABSTRACT

A new versatile hybrid nanocarrier has been designed using a "soft chemistry" synthesis, to efficiently encapsulate a photosensitizer – the protoporphyrin IX (Pp IX) – while preserving its activity intact in biological environment for advantageous use in photodynamic therapy (PDT). The synthesized Pp IX silica-based nanocarriers show to be spherical in shape and highly monodisperse with size extending from 10 nm up to 200 nm according to the synthesis procedure. Upon laser irradiation, the entrapped Pp IX shows to efficiently deliver reactive oxygen species (ROS) which are responsible for damaging tumor tissues. The ability of Pp IX silica-based nanocarriers to induce tumor cell death has been tested successfully *in vitro*. The stability of the Pp IX silica-based nanocarriers has been followed by UV–vis absorption and fluorescence emission in aqueous media and in 100% mouse serum media. The flexibility of the nanocarrier silica core has been examined as the key parameter to tune the Pp IX stability in biological environment. Indeed, an additional biocompatible inorganic surface coating performed on the Pp IX silica-based nanocarriers to produce an optimized bilayer coating demonstrates to significantly enhance the Pp IX stabilization in biological environments. Such versatile hybrid nanocarriers open new perspectives for PDT.

1. Introduction

Photodynamic therapy (PDT) is now a well established therapy which is used to treat various diseases, including cancer and more particularly superficial human cancer [1–5]. Photodynamic therapy requires three elements: light, a photosensitizer (PS) and oxygen. When the photosensitizer is exposed to specific wavelengths of light, it becomes activated from a ground to an excited state. As it returns to the ground state, it releases energy, which is transferred to oxygen to generate reactive oxygen species (ROS), such as singlet oxygen and free radicals. These ROS mediate cellular toxicity.

First-generation photosensitizers are hematoporphyrin, its derivative (HpD), and the purified commercially available Photofrin™. The first clinical PDT was performed in patients with bladder or skin cancer using HpD. In 1993, Photofrin™ (Porfimer sodium) became the first photosensitizer to be approved for PDT for recurrent, superficial papillary bladder cancer. It is still the most widely used and studied photosensitizer [3].

However, porfimer sodium has a long half-life for plasma elimination in all explored species including humans. It is retained for long periods in tissues other than the tumor structure [6–9]. The major late effect is skin photosensitization for up to 4–6 weeks after Photofrin™ injection [10].

At present, it is commonly admitted that the ideal photosensitizer would be a chemically stable and pure drug with preferential uptake in tumor, rapid clearance, and a strong absorption peak at light wavelengths >630 nm. Above all, a low toxicity and a high selectivity is the primary end point highlighted by clinicians [11].

In addition to development of new photosensitizers that efficiently absorb light at longer wavelength, significant efforts are still carried out to improve the localization of the photosensitizer to the tumor tissue. Further target specificity can be also achieved by controlling the location at which light activates the drugs. Molecular Drug Delivery System (DDS) has been developed as a way to vehicle photosensitizers to the target tumor. Various delivery systems have been tested in preclinical models so far [12–15]. Photoimmunotargeting uses monoclonal antibodies that recognize tumor antigens [16]. Ligands against receptors that are upregulated in tumor cells could be another delivery vehicle [17,18]. Liposomes and immunoliposomes can also be used in conjunction with photosensitizers [19].

Currently, nanoparticles represent emerging photosensitizer delivery systems that show great promise for PDT [20,21]. Two types of nanoparticle strategies are investigated. Either biodegradable nanoparticles, from which photosensitizer may be released

* Corresponding author. Tel.: +33 1 40 26 04 70; fax: +33 1 40 26 44 04.
E-mail address: agnes.pottier@nanobiotix.com (A. Pottier).

1011-1344/$ - see front matter © 2010 Elsevier B.V. All rights reserved.
doi:10.1016/j.jphotobiol.2010.03.009

within the tissues [22–27], or "pure carriers" non-biodegradable nanoparticles which kept photosensitizer entrapped during their activity [28–33].

Based on these concepts, different nanoparticle chemistries have been developed in our platform to define the optimal components and the simplest structure of these products for intended use in the clinics. Indeed, most efforts have been focused on selecting one product which low complexity avoids as much as possible metabolic and tissue interactions and fulfills the following conditions:

(1) To keep the simplest synthesis route, avoiding the use of targeting agent but taking advantage of the "enhanced permeability and retention (EPR) effect" that tumor tissues offer. The EPR effect is based on two factors [34,35]. First, the capillary endothelium in malignant tissues is more disorderly and thus more permeable towards macromolecules than the capillary endothelium in normal tissues. This allows extravasation of circulating polymeric nanoparticles within the tumor interstitium. Second, the lack of tumor lymphatic drainage in the tumor bed results in drug accumulation.
(2) To keep stability – ability to produce ROS – of the encapsulated photosensitizer at least for the necessary time to accumulate within tumor tissues and to produce its effect upon light activation.

The protoporphyrin IX (Pp IX) has been chosen as photosensitizer for the present study as it can be obtained as a pure well characterized monomer species. No modification of the photosensitizer molecule was attempted to covalently link the photosensitizer to the nanoparticles. Instead, a physical encapsulation was performed with the will to simplify as much as possible both the product synthesis route and its final composition.

Simple synthesis was performed to generate Pp IX silica-based nanocarriers with bilayer coating, as photosensitizer vehicles with efficient stabilization in biological environments.

Specifically, this paper underlines the key synthesis parameters that may tune the size of the silica-based nanocarriers within the nanometer range. Furthermore, since loss of optical properties stability of the entrapped Pp IX upon aging in mouse serum was observed, addition of a second biocompatible inorganic coating to tune the flexibility resulted of the most relevance. Improvement of the optical properties stability of the Pp IX silica-based nanocarriers with bilayer coating was achieved with promising possibility of differential accumulation in tumors.

2. Materials and methods

2.1. Materials

Protoporphyrin IX (Pp IX), N-N-dimethylformamide (DMF), TWEEN-80, 1,3-diphenylisobenzofuran (DPIBF), sodium trimetaphosphate (STMP) and D-glucose 20% stock solution were all obtained from Sigma–Aldrich. 1-butanol and ammonia (35%) were obtained from Fisher. Triethoxyvinylsilane (VTES) and ethanol where obtained from Fluka. All starting materials were obtained at the highest purity level available and used without purification. Sterile PBS 10× solution and fetal calf serum (FCS) were obtained from Invitrogen. Mouse serum was obtained from PAA laboratories.

2.2. Preparation of the Pp IX silica-based nanocarriers

In a typical experiment, the micelles were prepared by dissolving TWEEN-80 (5.5 g) and 1-butanol (6 mL) in ultra pure water (200 mL) under vigorous magnetic stirring. Ammonia (10 M, 200 μL) was added. The resulting clear solution was then transferred in a reactor (250 mL double layer glass reactor from Bercauverre-France, equipped with a stirrer from Fisher-Bioblock). The solution was allowed to stabilize at a temperature of 27 ± 0.5 °C under stirring. Pp IX in DMF (71.6 mM, 1.5 mL) was dissolved in solution. Neat triethoxyvinylsilane (2 mL) was added to the micellar system, and the resulting solution was stirred for about 24 h. At the end of the process, surfactant TWEEN-80 and cosurfactant 1-butanol were removed by dialyzing the solution against cold water (4 °C) in a 12–14 kDa cutoff cellulose membrane (Cellusep T 3-45-15, from Interchim). The dialysis water was changed once a day for 120 h. The dialyzed solution was then concentrated by a factor about 10 using an ultrafiltration device (Amicon stirred cell model 8400 from Millipore) with a 30 kDa cellulose membrane. The resulting solution was ultimately filtered through a 0.22 μm cutoff membrane filter (PES membrane from Millipore) under laminar hood. Sterilized PBS 10X solution (1 mL) was added to the as prepared sterilized solution (9 mL) under laminar hood and used for further experimentation.

2.3. Adjustment of the Pp IX silica-based nanocarriers size

The size of Pp IX silica-based nanocarriers has been tuned within the nanometer range by switching the temperature of the double layer glass reactor from 18 ± 0.5 °C up to 37 ± 0.5 °C, keeping all others synthesis parameters constant. Subsequently, the cosurfactant (1-butanol) content has been increased from 6 mL up to 10 mL to bring an additional control of nanocarrier size. For the largest nanocarriers size, the volume of triethoxyvinylsilane was however increased to ensure an efficient entrapment of the Pp IX molecules within the silica-based nanocarriers.

2.4. Preparation of the STMP-modified Pp IX silica-based nanocarriers

In a typical experiment, Pp IX silica-based nanocarriers in aqueous suspension (2.5 ± 0.5 mM Pp IX, 1 mL) were mixed with STMP aqueous solution (500 mg mL^{-1}). The volume of STMP aqueous solution added was the following: sample A (116.5 μL), sample B (46.5 μL) and sample C (31 μL). The resulting solutions were adjusted to pH 7 ± 0.1 and maintained under mild agitation overnight. D-glucose 20% stock solution (0.335 mL) was then added to the solution. The solution was ultimately filtered through a 0.22 μm cutoff membrane filter (PES membrane from Millipore) and used as such for stability studies and *in vitro* assays.

2.5. Characterizations

Transmission electron microscopy (TEM) was employed to determine the morphology and size of the aqueous dispersion of Pp IX silica-based nanocarriers, using a JEOL 100 CX electron microscope, operating at an accelerated voltage of 100 kV. UV–vis absorption spectra were recorded using a VARIAN Cary 100 Scan spectrophotometer, in a quartz cuvette with 0.2 mm path length. Fluorescence spectra were recorded on a VARIAN Cary Eclipse fluorescence spectrophotometer equipped with a 96 well microplate. HPD7404 Laser Driver System from Intense Ltd., with diodes 635 ± 3 nm was used for detection of singlet oxygen generation following Pp IX irradiation.

2.6. Determination of Pp IX concentration

The concentration of Pp IX in the different media – free Pp IX (dispersed in DMF solvent) or Pp IX entrapped within nanocarriers – was determined from maximum optical density of the soret band positioned at 405 nm.

2.7. Detection of singlet oxygen

The generation of singlet oxygen was determined chemically, using 1,3-diphenylisobenzofuran (DPIBF) as a singlet oxygen detection probe. DPIBF is bleached by singlet oxygen to its corresponding endoperoxide [26]. The reaction was monitored spectrophotometrically by recording the decrease in fluorescence intensity of DPIBF upon excitation at 412 nm.

In a typical experiment, a stock solution of DPIBF in ethanol (0.85 mM, 400 μL) was mixed with ethanol solution (4 mL). A corresponding volume of samples (Pp IX silica-based nanocarriers in PBS 1X solution or free Pp IX in DMF solvent) was then added to get a final concentration of Pp IX of 0.2 μM. The solutions were then transferred in a 96 well microplate and irradiated with a 635 ± 3 nm laser source. Preliminary experiments have been undertaken to optimize the laser intensity and the time of irradiation for an efficient generation of singlet oxygen, using free Pp IX in DMF solvent as reference. The following conditions have been retained corresponding to an energy delivered of 11.4 J cm^{-2}: I = 0.70 A for 69 s – I = 0.85 A for 24 s or I = 1.00 A for 15 s. Using alternatively one of the three conditions, a decrease of 50% of the fluorescence of DPIBF prior and after irradiation was observed, which was considered as relevant for further experimentation.

2.8. Stability studies in 100% mouse serum media

Stability of the Pp IX silica-based nanocarriers and STMP-modified Pp IX silica-based nanocarriers has been studied in 100% mouse serum media. In a typical experiment sterile sample, free Pp IX in DMF (2.5 mM Pp IX, 50 μL), Pp IX silica-based nanocarriers in PBS 1X solution (2.5 mM Pp IX, 50 μL) and STMP-modified Pp IX silica-based nanocarriers in 5% glucose solution (1.5 mM Pp IX, 50 μL) were mixed with mouse serum media (2.45 mL). The solutions were then incubated at 37 °C in a thermostated bath. UV–vis absorption spectra and fluorescence emission (405 nm excitation wavelength) of Pp IX were recorded up to 24 h prior and after filtration through a 0.22 μm cutoff membrane filter (PES membrane from Millipore).

2.9. Effects of Pp IX silica-based nanocarriers and STMP-modified Pp IX silica-based nanocarriers on tumor cell survival by WST-1 assay

The WST-1 cell viability assay (Roche Molecular Biochemicals; 11644703) is based on the cleavage of the tetrazolium salt, WST-1 (4-[3-(4-iodophenyl)-2-(4-nitrophenyl)-2*H*-5-tetrazolio]-1,3-benzene disulfonate), by mitochondrial dehydrogenases in viable cells to form highly water-soluble formazan (dark red) measured by absorbance UV.

Pp IX silica-based nanocarriers, STMP-modified Pp IX silica-based nanocarriers and free Pp IX, treated or not with light activation were tested. Human cell line HCT 116 (colon cancer cell line) was obtained from the American Type Culture Collection (ATCC-LGC Promochem, Molsheim, France). HCT 116 cells were maintained in Mc Coy's 5a medium with GlutaMAX supplemented with 10% (v/v) heat-inactivated fetal calf serum (FCS). Cells were maintained at 37 °C in the presence of 5% CO_2. Assays were performed in 96 well microplates. 12,000 cells were incubated in the presence of increasing concentrations of Pp IX (from 0.39 up to 100 μM), for 3 h at 37 °C. After incubation, medium was removed. Cells were rinsed once with PBS 1X and fresh complete medium was added. Cells were activated with red lamp at 630 nm during 20 min at room temperature – the red lamp device was designed in order to improve homogeneity of light dose when exposing 96 well microplates containing the tested cells. Briefly, it is composed of 88 diodes, each emitting light at 630 nm, organized on a plate (Intellibio, France). The total fluence of lamp is 15 mW cm^{-2}.

After 48 h, viability was assessed by WST-1 assay.

Cells were incubated for 2 h with WST-1 (10 μL) to achieve 1:10 final dilution. The absorbance of the converted dye was measured at a wavelength of 450 nm (BioTek, PowerWave 340). Cell viability rate was calculated based on the absorbance measured relative to that of control cultured cells. Viability of cells for all experimental group cells was determined in triplicate.

2.10. Effects of STMP-modified Pp IX silica-based nanocarriers on tumor cell survival by WST-1 assay, upon aging in 100% FCS media

The effect of STMP-modified Pp IX silica-based nanocarriers on tumor cell survival has been studied after aging the nanocarriers in 100% FCS media. In a typical experiment, STMP-modified Pp IX silica-based nanocarriers in 5% glucose solution (1.5 ± 0.5 mM Pp IX, 40 μL) were mixed with FCS media (160 μL). The solutions were then incubated at 37 °C in a thermostated bath for respectively t = 0 h (no aging), t = 5 h aging and t = 12 h aging. At the end of the incubation period, the solutions were mixed with Mc Coy's 5a medium with GlutaMAX (800 μL). The ability of the resulting STMP-modified Pp IX silica-based nanocarriers suspension to kill cells *in vitro* was tested by WST-1 assay, as detailed here above.

3. Results and discussion

3.1. Pp IX silica-based nanocarriers

The Pp IX silica-based nanocarriers are synthesized in the non polar core of TWEEN-80/1-butanol/water micelles using triethoxyvinylsilane as silica precursor.

A TEM image of Pp IX silica-based nanocarriers is shown in Fig. 1. The silica-based nanocarriers are spherical, having uniform size distribution, with an average size of 25 nm.

The UV–vis absorption and fluorescence emission spectra (excitation wavelength 405 nm) of free Pp IX in DMF and Pp IX silica-based nanocarriers in aqueous solution (46 μM Pp IX) are similar (Fig. 2), indicating no changes in Pp IX upon entrapment within nanocarriers.

However, the same concentration of free Pp IX in 2% DMF/water solution exhibits a poorly resolved absorption spectrum (Fig. 2) and a complete loss of fluorescence emission.

The modification of absorption spectrum of the Pp IX in a polar solvent and the corresponding loss of fluorescence emission may be due to either Pp IX – solvent interaction resulting in non radiative decay or Pp IX self – aggregation in a polar solvent leading to fluorescence quenching.

It is worth noting that Pp IX silica-based nanocarriers in aqueous solution do not present such behavior. Hence, the Pp IX molecules may be envisaged as discretely embedded in the silica-based

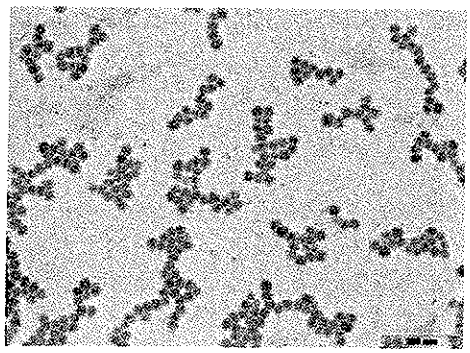

Fig. 1. TEM image of Pp IX silica-based nanocarriers. TEM image shows particles with an average diameter of 25 nm and a uniform size distribution.

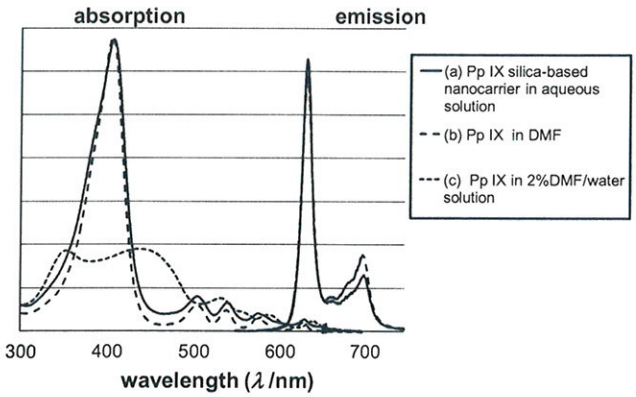

Fig. 2. UV–vis absorption and emission spectra of Pp IX. UV–vis absorption and emission (excitation wavelength 405 nm) spectra of (a) Pp IX in DMF, (b) Pp IX silica-based nanocarriers in aqueous solution, and (c) Pp IX in 2% DMF/water solution. Pp IX concentration 46 μM.

nanocarriers as proposed in Scheme 1a and therefore protected from exposure to aqueous environment, preventing a loss of fluorescence. Indeed, the hydrophobic vinyl group of the silica precursor is believed to effectively confine the Pp IX photosensitizer within the silica core, protecting the photosensitizer from aqueous environment. The data strongly support the interest of such silica-based nanocarriers as efficient carriers for drugs to protect the drug from exposure to aqueous environment.

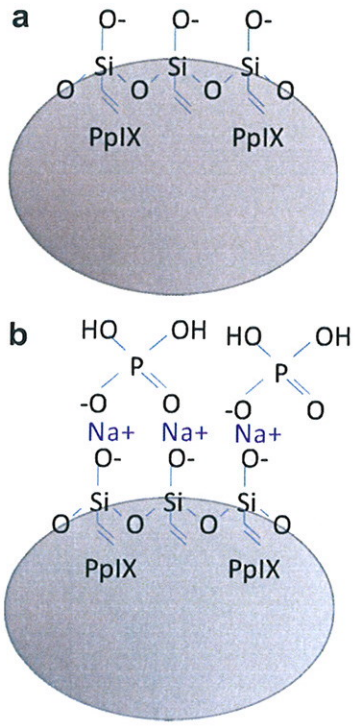

Scheme 1. Schematic illustration of Pp IX silica-based-nanocarriers and STMP-modified Pp IX silica-based nanocarrier. (a) Schematic illustration of Pp IX silica-based nanocarrier. The hydrophobic vinyl group of the silica precursor is believed to effectively confine the Pp IX photosensitizer within the silica core, protecting the photosensitizer from aqueous environment. (b) Schematic illustration of STMP-modified Pp IX silica-based nanocarrier. The phosphate bilayer coating is believed to bring an effective protection of the Pp IX molecule upon exposure to biological environment by reducing the flexibility of the silica core, due to specific electrostatic interactions which are developed between the silanol groups of the silica precursor and the phosphate groups of the STMP compound, mediated by sodium counter-ion.

Detection of singlet oxygen generation by chemical method was performed with two samples (free Pp IX in DMF solvent and Pp IX silica-based nanocarriers in PBS 1X solution) at 0.2 μM Pp IX concentration. Fig. 3 presents the decrease of DPIBF fluorescence for a given energy (11.4 J cm^{-2}) using three different laser intensity conditions and adjusting the time of light exposure accordingly. A similar decrease of DPIBF fluorescence was observed for both samples, indicating the generation of singlet oxygen with similar efficiencies in both cases.

The data show that the silica-based nanocarriers present a relevant range of porosity in aqueous solution to efficiently entrapped the Pp IX photosensitizer – pore sizes are too small to allow the drug to escape the matrix – while preserving Pp IX photosensitizer ability to interact with molecular oxygen which has diffused through the pores – pore sizes are large enough to enable efficient oxygen diffusion to and from the nanocarrier. This can lead to the formation of singlet oxygen by energy transfer from the excited Pp IX to molecular oxygen, which can then diffuse out of the nanocarrier to produce its effect.

The ability of the Pp IX silica-based nanocarriers to generate singlet oxygen after previous light activation was investigated.

No physical degradation of the Pp IX silica-based nanocarriers is observed following drastic laser irradiation (320 J cm^{-2}, laser intensity 1 A for 420 s) (Fig. S1, Supporting Information). Furthermore, detection of singlet oxygen generation by chemical method on the resulting twice irradiated Pp IX silica-based nanocarriers sample shows an interesting ability to generate singlet oxygen (Fig. 3).

The data strengthen the potential of such silica-based nanocarriers to preserve the photosensitizer properties following multiple light activations.

In vitro viability assays on HCT 116 cell line have been performed for 2 different samples (free Pp IX in DMF solvent and Pp IX silica-based nanocarriers in PBS 1X solution). No significant dark toxicity was observed for any samples. On contrast, the photosensitizer appears effective in a dose-dependent manner under light irradiation. EC_{50} determined for Pp IX in DMF solvent and for Pp IX silica-based nanocarriers in PBS 1X solution are respectively of 6.03 μM ± 0.43 and 0.44 ± 0.05 μM (Fig. S2, Supporting Information). Of note, no dark toxicity (without irradiation), nor efficacy (with light irradiation) of the silica-based nanocarrier without Pp IX entrapped was observed in any tested conditions (data not shown).

The data show that Pp IX silica-based nanocarrier is an effective drug-carrier system for killing cells *in vitro* after light exposure.

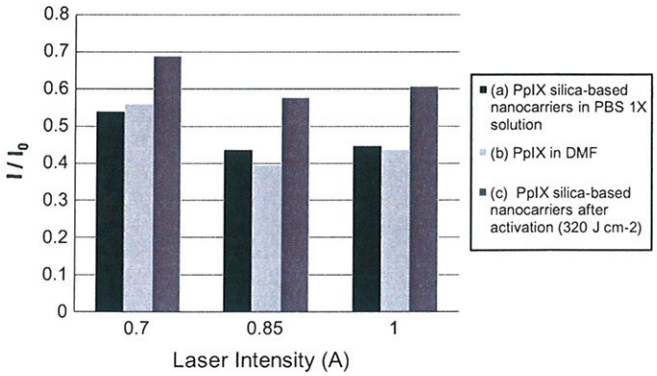

Fig. 3. Decrease of DPIBF fluorescence upon laser irradiation. (a) Pp IX silica-based nanocarriers in PBS 1X solution, (b) Pp IX in DMF solvent, and (c) Pp IX silica-based nanocarriers in PBS 1X solution following laser activation (320 J cm^{-2}, 1 A, 420 s). For all compounds, Pp IX concentration was 0.2 μM. Data are expressed as I/I_0 ratio (I_0: initial DPIBF fluorescence, I: DPIBF fluorescence upon laser irradiation).

3.2. Adjustment of the size of the Pp IX silica-based nanocarriers

Fig. 4 shows the TEM images of Pp IX silica-based nanocarriers in aqueous solution synthesized by varying the temperature of the double layer glass reactor between 18 ± 0.5 °C and 37 ± 0.5 °C and the volume of cosurfactant between 6 mL and 10 mL, all others synthesis parameters being constant. For the largest nanocarriers size, the volume of triethoxyvinylsilane was however increased to ensure an efficient entrapment of the Pp IX molecules within the silica-based nanocarriers. Indeed, the stability of optical properties of the encapsulated Pp IX has been controlled by recording the UV–vis absorption and the fluorescence emission spectra (excitation wavelength 405 nm) of the as prepared Pp IX silica-based nanocarriers in aqueous media (data not shown). Further, Pp IX payload was similar for all the nanocarriers.

Control of the size of the Pp IX silica-based nanocarriers may be tuned from 10 nm (T = 18 ± 0.5 °C and 1-butanol = 6 mL) up to 200 nm (T = 37 ± 0.5 °C and 1-butanol = 10 mL) with uniform particle size.

We do not know the precise mechanisms which alter the micelles structure: both the temperature and cosurfactant content may affect simultaneously the structure of the micelles. Indeed, the Critical Micellar Concentration (CMC) of the TWEEN-80 is known to be temperature dependant. Additionally, an increase of cosurfactant amount could allow blowing up the micelles. Moreover, ethanol produced during the hydrolysis of triethoxyvinylsilane may affect the micelles structure [36]. The understanding of each parameter role and its impact on micelles structure is out of scope of this paper. More experiments are needed to explore this topic.

Whatever the size of the Pp IX silica-based nanocarriers, *in vitro* viability assays on HCT 116 cell line show similar efficacy for tumor cell death upon light irradiation [37].

The results demonstrate that the size of Pp IX silica-based nanocarriers may be adjusted within the nanometer range – from 10 nm up to 200 nm – by tuning either the temperature and/or the cosurfactant content during the synthesis, with no loss of the encapsulated Pp IX properties. These observations illustrate the potential of silica-based nanocarriers to successfully encapsulate drugs using the size of the nanocarriers as key parameter to control the biodistribution for a self and efficient trafficking to tumor tissues *in vivo*. Further studies should be undertaken to evaluate the maximum of drugs uptake within the nanocarrier as a function of its size.

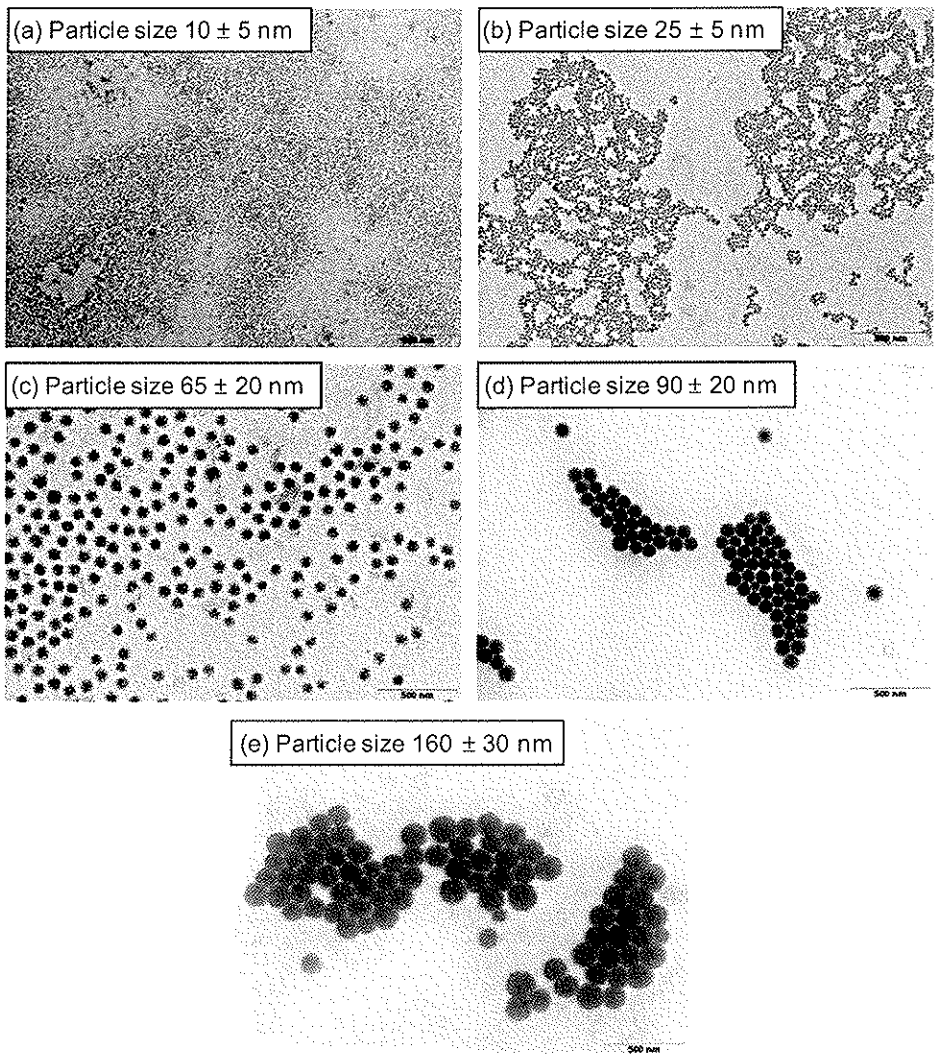

Fig. 4. TEM images of Pp IX silica-based nanocarriers in aqueous solution showing the ability to tune the size of the nanocarriers within the nanometer range (from 10 up to 200 nm) with a uniform particle size distribution. (a) T = 18 ± 0.5 °C, 1-butanol = 6 mL, VTES = 2 mL; (b) T = 27 °C ± 0.5 °C, 1-butanol = 6 mL, VTES = 2 mL; (c) T = 37 °C ± 0.5 °C, 1-butanol = 6 mL, VTES = 2 mL; (d) T = 37 °C ± 0.5 °C, 1-butanol = 8 mL, VTES = 6 mL; (e) T = 37 °C ± 0.5 °C, 1-butanol = 10 mL, VTES = 6 mL. Scale bar 500 nm.

3.3. Pp IX silica-based nanocarriers stability study in 100% mouse serum media and design and synthesis of STMP-modified Pp IX silica-based nanocarriers

Stability study of Pp IX entrapped within silica-based nanocarriers, has been followed by UV–vis absorption and fluorescence emission of the Pp IX molecule.

No modification of the absorption and no decay of the fluorescence emission of Pp IX entrapped within silica-based nanocarriers have been observed upon storage in PBS 1X solution.

On contrast, Pp IX entrapped within silica-based nanocarrier presents a modification of its absorption spectrum after $t = 2$ h aging in 100% mouse serum media at 37 °C (Fig. 5a). A corresponding loss of fluorescence emission and a shift of the 630 nm emission peak are observed (Fig. 5b).

It is worth noting that Pp IX in DMF, on contact with mouse serum media at 37 °C, presents the same modification of absorption spectrum already at $t = 0$ h (no aging). A corresponding loss of fluorescence emission with a shift of the 630 nm emission peak is also observed upon aging (Fig. S3, Supporting Information). Most photosensitizer molecules such as Pp IX are hydrophobic and can aggregate easily in aqueous media, which can affect their photophysical, chemical and biological properties [20]. The modification of absorption spectrum of the Pp IX on contact with mouse serum media and the corresponding loss of fluorescence emission may be due to either Pp IX – biological media interaction resulting in non radiative decay or Pp IX self – aggregation in biological media leading to fluorescence quenching.

Despite an improved stability of the Pp IX entrapped within silica-based nanocarriers in 100% mouse serum media as compared to Pp IX in DMF on contact with mouse serum media at 37 °C, there is a need to further improved the stability – ability to produce ROS – of the encapsulated photosensitizer at least for the necessary time to accumulate within tumor tissues and to produce its effect upon light activation.

Observation of the Pp IX silica-based nanocarriers after $t = 24$ h aging at 37 °C in 100% mouse serum media reveals not alteration of the nanocarriers structure which suggests that no degradation of the nanocarriers has occurred (Fig. S4, Supporting Information).

The integrity of the silica-based nanocarrier upon aging in 100% mouse serum media strengthens the hypothesis that an adjustment of the flexibility, hence the permeability, of the silica core is fundamental to improve the stability of the entrapped Pp IX. Roach et al. [38] have reported protein adsorption (BSA and fibrinogen) onto model hydrophobic (CH_3) and hydrophilic (OH) surfaces. Their data showed that albumin undergoes adsorption via a single step whereas fibrinogen adsorption is a more complex, multistage process. Albumin has a stronger affinity toward the CH_3 compared to OH terminated surface. In contrast fibrinogen adheres more rapidly to both surfaces, having a slightly higher affinity toward the hydrophobic surface. Conformational assessment of the adsorbed proteins shows that after initial first hour incubation few further time-dependent changes are observed. Both proteins exhibited a less secondary structure upon adsorption onto a hydrophobic surface than onto a hydrophilic surface, with the effect observed greatest for albumin. Data presented in this article suggest that proteins (albumin and fibrinogen) are able to interact with hydrophilic surface and show a stronger affinity with hydrophobic surface. Their adsorption may further induce a conformational change in protein structure. In our present study, interaction of silica-based nanocarriers and protein from serum is likely to occur. Albumin is the most abundant protein in serum and it is suggested that its interaction with hydroxyl group of silica-based nanocarriers readily occurs. However, the three dimensional structure of the nanocarrier backbone present some flexibility and hydrophobic vinyl groups, initially constraint within the core of the nanocarrier upon exposure to aqueous environment, may get oriented toward the external surface, triggered by albumin, upon exposure with serum media. Such affinity – vinyl hydrophobic groups and albumin – could be an explanation for the loss of stability of the entrapped Pp IX which may become exposed to the serum media. To support this hypothesis, a second biocompatible inorganic surface coating has been performed in order to tune the flexibility of the silica-based nanocarriers core. For this, sodium trimetaphosphate (STMP) compound has been chosen. Indeed, STMP is a biocompatible phosphate compound with FDA approval.

Phosphate compounds, such as sodium trimetaphosphate are considered as complexing agent for most oxide surface. However, silica surface behaves differently. Furthermore, both silica surface and sodium trimetaphosphate are negatively charged at neutral pH. We hypothesized that sodium cations, present in the solution, drive the interaction between phosphate compound and silica-based nanocarriers silanol surface groups as proposed in Scheme 1b, hence confining the hydrophobic vinyl groups and therefore the hydrophobic Pp IX photosensitizers within the nanocarriers core.

Furthermore, STMP compound may be added at the end of the process and will not interfere with the silica-based nanocarriers synthesis. Hence, ultimate surface modification of the silica-based nanocarriers may be controlled according to its intended use and in a well reproducible manner.

Indeed, the UV–vis absorption spectra of the STMP-modified Pp IX entrapped within silica-based nanocarriers show limited

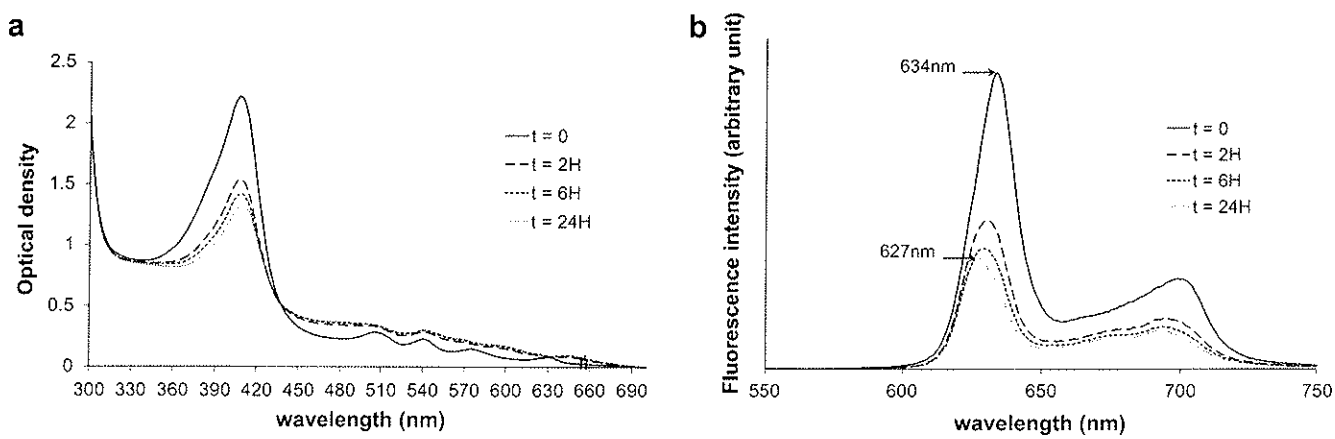

Fig. 5. UV–vis absorption and emission spectra of Pp IX silica-based nanocarrier upon aging in mouse serum media: (a) UV–vis absorption spectra and (b) corresponding fluorescence emission spectra (excitation wavelength 405 nm) of Pp IX silica-based nanocarriers upon aging at 37 °C in 100% mouse serum media.

modifications upon aging in 100% mouse serum media with the 630 nm absorption peak being still apparent after $t = 5$ h aging (Fig. S5, Supporting Information).

Table 1 presents the stability of Pp IX optical properties results after $t = 5$ h aging at 37 °C of the STMP-modified Pp IX silica-based nanocarriers in 100% mouse serum media with increase amount of STMP. Pp IX concentration of the STMP-modified Pp IX silica-based nanocarriers in aqueous solution is taken as reference. Pp IX concentration of the STMP-modified Pp IX silica-based nanocarriers in 100% mouse serum media at $t = 0$ h (no aging), and $t = 5$ h aging after filtration on a 0.22 μm cutoff membrane filter are reported. We assumed that we can calculate the real UV–vis absorption of the Pp IX entrapped within the nanocarriers by measuring the absorption spectrum of the suspension and subtracting the baseline scattering from mouse serum. Stability recovery (expressed in %) is determined by performing the ratio between optical densities at the maximum of the Soret peak at $t = 5$ h aging after filtration and $t = 0$ h (no aging), in 100% mouse serum media.

Table 1
Stability results of STMP-modified Pp IX silica-based nanocarriers upon aging in mouse serum media Pp IX concentration of STMP-modified Pp IX silica-based nanocarriers in aqueous solution. Pp IX concentration of STMP-modified Pp IX silica-based nanocarriers in 100% mouse serum media at 37 °C: $t = 0$ h (no aging), $t = 5$ hours aging after 0.22 μm filtration. Stability recovery. For sample A, B and C, the volume of STMP aqueous solution (500 mg mL^{-1}) added was respectively of 116.5 μL, 46.5 μL and 31 μL.

	[Pp IX] in aqueous media (mM)	[Pp IX] in mouse serum media $t = 0$ h (mM)	[Pp IX] in mouse serum media $t = 5$ h + filtration (mM)	Stability recovery (%)
STMP-modified silica-based nanocarriers				
Sample A	1.04	1.00	0.80	80
Sample B	1.45	1.55	1.20	77
Sample C	2.05	2.07	1.35	65
Silica-based nanocarriers	2.88	2.85	1.04	37

The data show that an increase amount of STMP added to the Pp IX silica-based nanocarriers results in an increase of the photosensitizer stability upon aging in 100% mouse serum media.

The role of STMP would then to stiffen the silicone backbone of the silica-based nanocarrier by forcing the silanol groups to interact with the phosphate groups, likely via sodium counter ions. Hence, confining the hydrophobic vinyl groups within the core of the nanocarrier and stabilizing the Pp IX molecules.

To confirm the ability of the bilayer nanocarriers system to kill tumor cells, *in vitro* viability assays were undertaken after aging the STMP-modified Pp IX silica-based nanocarriers in 100% FCS media. FCS media has been chosen for *in vitro* studies due to the intrinsic toxicity of mouse serum media on human cell lines. The

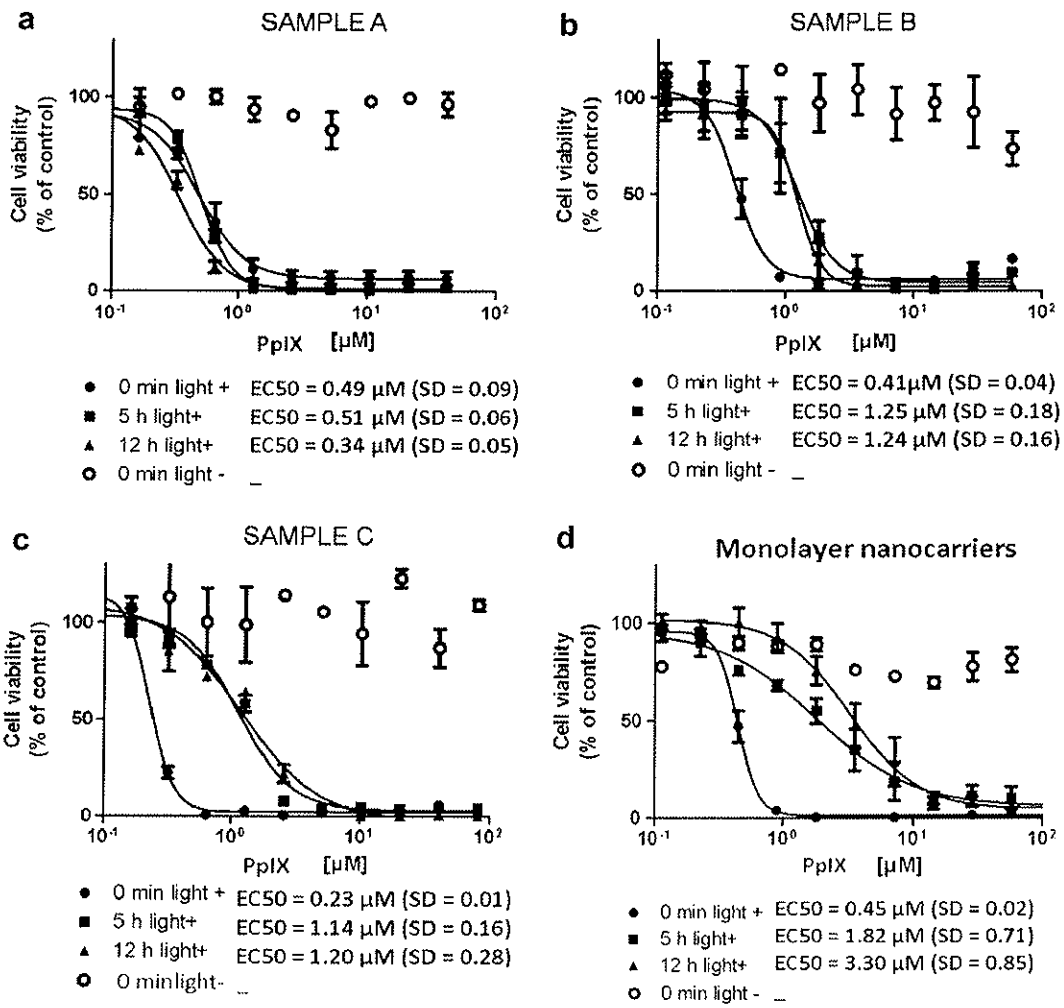

Fig. 6. In vitro viability assays. Effect of STMP content (STMP 500 mg mL^{-1}) on *in vitro* viability assays on HCT 116 upon aging the nanocarriers solutions in 100% FCS media at 37 °C. STMP-modified Pp IX silica-based nanocarriers: (a) sample A (volume of STMP = 116.5 μL); (b) sample B (volume of STMP = 46.5 μL); (c) sample C (volume of STMP = 31 μL); and (d) Pp IX silica-based nanocarriers. All the nanocarriers are in 5% glucose solution.

phototoxicity brought by the bilayer nanocarriers is manifest, as shown in Fig. 6. Furthermore, an increase amount of STMP significantly preserves the ability of the Pp IX silica-based nanocarriers to kill cell after aging in 100% FCS media. Furthermore, no toxicity (without irradiation), nor efficacy (with light irradiation) of the STMP-modified silica-based nanocarrier without Pp IX entrapped was observed in any tested conditions (data not shown). Despite a drop of the EC_{50} value observed in the five first hours for the lowest STMP content (Fig. 6b and c), no further evolution is observed up to 12 h.

Hence, a second biocompatible inorganic surface coating to control the flexibility, hence the permeability, of the Pp IX silica-based nanocarriers core is shown to be an efficient way to improve the stability of the nanocarriers in biological media. Moreover, the present *in vitro* study – performed up to 12 h aging – suggests that efficacy may be preserved for enough time to allow the nanocarriers accumulation within tumor tissues and produce its effect upon light irradiation.

4. Conclusions

In this paper, we demonstrate that the use of a "soft chemistry" synthesis allows designing a new versatile hybrid nanocarrier with promising opportunity for PDT.

This nanocarrier is expected to reach one of the key challenges of the domain by allowing the delivery of the nanotherapeutic at the right time, at the right site and at the right dose.

Advantageously, the present work shows that the size of the silica-based nanocarriers may be tuned within the nanometer range – from 10 nm up to 200 nm – by adjusting either the temperature of the process or the cosurfactant amount. Hence, the size of the nanocarriers may be adjusted for efficient biodistribution. Furthermore, it is anticipated that the amount of entrapped drugs could be adapted to precisely achieve the right dose *in vivo*. Further work should be undertaken to confirm this hypothesis.

Upon laser irradiation, the entrapped Pp IX has shown to efficiently deliver ROS and multiple light activations may be envisaged to enhance efficacy of the Pp IX silica-based nanocarriers system.

Of particular importance, we have shown that the addition of STMP to the Pp IX silica-based nanocarriers at the end of the process allows tuning the Pp IX stability upon aging in mouse serum media. Besides, *in vitro* viability assays performed after aging the STMP-modified Pp IX silica-based nanocarriers in 100% FCS media at 37 °C, validate the stability – ability to produce ROS – of the encapsulated photosensitizer up to 12 h. Preliminary *in vivo* studies in tumor-bearing animals, performed with Pp IX silica-based nanocarriers, the monolayer nanocarriers, have shown efficient accumulation within tumors [37]. Further, kinetics demonstrated by semiquantitative analysis showed that tumor models behaved differently according to the maximal accumulation time point.

The second generation of nanocarriers, the STMP-modified Pp IX silica-based nanocarriers, anticipate promises for efficient *in vivo* efficacy, due to their enhance stability – ability of the entrapped photosensitizers to generate ROS upon laser light excitation – in biological environment. Experiments to evaluate the performance and safety of this new drug-bilayer nanocarriers system in *in vivo* models will be performed.

5. Abbreviations

Pp IX	protoporphyrin IX
PDT	photodynamic therapy
ROS	reactive oxygen species
PS	photosensitizer
DDS	drug delivery system

Appendix A. Supplementary material

Supplementary data associated with this article can be found, in the online version, at doi:10.1016/j.jphotobiol.2010.03.009.

References

[1] T.J. Dougherty, C.J. Gomer, B.W. Henderson, G. Jori, D. Kessel, M. Korbelik, J. Moan, G. Peng, Photodynamic therapy, J. Natl. Cancer Inst. 90 (1998) 889–905.
[2] C.H. Sibata, V.C. Colussi, N.L. Oleinick, T.J. Kinsella, Photodynamic therapy: a new concept in medical treatment, Braz. J. Med. Biol. Res. 33 (2000) 869–880.
[3] M. Triesscheijn, P. Baas, J.H.M. Schellens, F.A. Stewart, Photodynamic therapy in oncology, The Oncologist 11 (2006) 1034–1044.
[4] D.E.J.G.J. Dolmans, D. Fukumura, R.K. Jain, Photodynamic therapy for cancer, Nat. Rev. Cancer 3 (2003) 380–387.
[5] R. Bonnet, Photosensitizer of the porphyrin and phthalocyanine series for photodynamic therapy, Chem. Soc. Rev. 24 (1995) 19–33.
[6] B.F. Overholt, K.K. Wang, J.S. Burdick, C.J. Lightdale, M. Kimmey, H.R. Nava, M.V. Sivak, N. Nishioka, H. Barr, N. Marcon, M. Pedrosa, M.P. Bronner, M. Grace, M. Depot, Five-year efficacy and safety of photodynamic therapy with photofrin in Barrett's high-grade dysplasia, Gastrointest. Endosc. 66 (2007) 460–468.
[7] S.A. Pahernik, M. Dellian, F. Berr, A. Tannapfel, Ch. Wittekind, A.E. Goetz, Distribution and pharmacokinetics of Photofrin® in human bile duct cancer, J. Photochem. Photobiol. B: Biol. 47 (1998) 58–62.
[8] L.-B. Li MD, R.-C. Luo, W.-J. Liao, M.-J. Zhang, Y.-L. Luo, J.-X. Miao, Clinical study of photofrin photodynamic therapy for the treatment of relapse nasopharyngeal carcinoma, Photodiagn. Photodyn. Ther. 3 (2006) 266–271.
[9] A. Orenstein, G. Kostenich, L. Roitman, Y. Shechtman, Y. Kopolovic, B. Ehrenberg, Z. Malik, Comparative study of tissue distribution and photodynamic therapy selectivity of chlorin e6, Photofrin II and ALA-induced protoporphyrin IX in a colon carcinoma model, Br. J. Cancer 73 (1996) 937–944.
[10] C.H. Sibata, V.C. Colussi, N.L. Oleinick, T.J. Kinsella, Photodynamic therapy in oncology, Expert Opin. Pharmacother. 2 (2001) 917–927.
[11] Z. Huang, A review of progress in clinical photodynamic therapy, Technol. Cancer Res. Treat. 4 (2005) 283–293.
[12] J.G. Christie, U.D. Kompella, Ophthalmic light sensitive nanocarrier systems, Drug Discov. Today 13 (2008) 124–134.
[13] K. Baba, H.E. Pudavar, I. Roy, T.Y. Ohulchanskyy, Y. Chen, R. Pandey, P.N. Prasad, A new method for delivering a hydrophobic drug for photodynamic therapy using pure nanocrystal form of the drug, Mol. Pharm. 4 (2007) 289–297.
[14] Y. Cheng, A.C. Samia, J.D. Meyers, I. Panagopoulos, B. Fei, C. Burda, Highly efficient drug delivery with gold nanoparticle vectors for *in vivo* photodynamic therapy of cancer, J. Am. Chem. Soc. 130 (2008) 10643–10647.
[15] A. Vaidya, Y. Sun, Y. Feng, L. Emerson, E.-K. Jeong, Z.-R. Lu, Contrast-enhanced MRI-guided photodynamic cancer therapy with a pegylated bifunctional polymer conjugate, Pharm. Res. 25 (2008) 2002–2011.
[16] M.B. Vrouenraets, G.W.M. Visser, F.A. Stewart, M. Stigter, H. Oppelaar, P.E. Postmus, G.B. Snow, G.A.M.S. Van Dongen, Development of *meta*-tetrahydroxyphenylchlorin-monoclonal antibody conjugates for photoimmunotherapy, Cancer Res. 59 (1999) 1505–1513.
[17] Y.N. Konan, R. Gurny, E. Allémann, State of the art in the delivery of photosensitizers for photodynamic therapy, J. Photochem. Photobiol. B: Biol. 66 (2002) 89–106.
[18] S. Ballut, A. Makky, B. Loock, J.-P. Michel, P. Maillard, V. Rosilio, New strategy for targeting of photosensitizers, synthesis of glycodendrimeric phenylporphyrins incorporation into a liposome membrane and interaction with a specific lectin, Chem. Commun. 2 (2009) 224–226.
[19] A.M. Richter, E. Waterfield, A.K. Jain, A.J. Canaan, B.A. Allison, J.G. Levy, Liposomal delivery of a photosensitizer benzoporphyrin derivative monoacid ring A (BPD) to tumor tissue in a mouse tumor model, Photochem. Photobiol. 57 (1993) 1000–1006.
[20] D. Bechet, P. Couleaud, C. Frochot, M.-L. Viriot, F. Guillemin, M. Barberi-Heyob, Nanoparticles as vehicles for delivery of photodynamic therapy agents, Trends Biotechnol 26 (2008) 612–621.
[21] S.A. Sibani, P.A. McCarron, A.D. Woolfson, R.F. Donnelly, Photosensitiser delivery for photodynamic therapy. Part 2: systemic carrier platforms, Expert Opin. Drug Deliv. 11 (2008) 1241–1254.
[22] Y.N. Konan, J. Chevallier, R. Gurny, E. Allémann, Encapsulation of p-THPP into nanoparticles: cellular uptake subcellular localization and effect of serum on photodynamic activity, Photochem. Photobiol. 77 (2003) 638–644.
[23] B. Pegaz, E. Debefve, J.-P. Ballini, Y.N. Konan-Kouakou, H. van den Bergh, Effect of nanoparticle size on the extravasation and the photothrombic activity of *meso* (p-tetracarboxyphenyl)porphyrin, J. Photochem. Photobiol. B: Biol. 85 (2006) 216–222.
[24] B. Pegaz, E. Debefve, F. Borle, J.-P. Ballini, H. van den Bergh, Y.N. Konan-Kouakou, Encapsulation of porphyrins chlorins in biodegradable nanoparticles: the effect of dye lipophilicity on the extravasion the photothrombic activity, a comparative study, J. Photochem. Photobiol. B: Biol. 80 (2005) 19–27.
[25] Y. Li, W.-D. Jang, N. Nishiyama, A. Kishimura, S. Kawauchi, Y. Morimoto, S. Miake, T. Yamashita, M. Kikuchi, T. Aida, K. Kataoka, Dendrimer generation effects on photodynamic efficacy of dendrimer porphyrins and dendrimer-loaded supramolecular nanocarriers, Chem. Mater. 19 (2007) 5557–5562.

[26] G.R. Reddy, M.S. Bhojani, P. McConville, J. Moody, B.A. Moffat, D.E. Hall, G. Kim, Y.-E.L. Koo, M.J. Woolliscroft, J.V. Sugai, T.D. Johnson, M.A. Philbert, R. Kopelman, A. Rehemtulla, B.D. Ross, Vascular targeted nanoparticles for imaging and treatment of brain tumors, Clin. Cancer Res. 12 (2006) 6677–6686.
[27] D. Gao, H. Xu, M.A. Philbert, R. Kopelman, Ultrafine hydrogel nanoparticles: synthetic approach and therapeutic application in living cells, Angew. Chem. Int. Ed. 46 (2007) 2224–2227.
[28] L.M. Rossi, P.R. Silva, L.L.R. Vono, A.U. Fernandes, D.B. Tada, M.S. Baptista, Protoporphyrin IX nanoparticle carrier: preparation optical properties and singlet oxygen generation, Langmuir 24 (2008) 12534–12538.
[29] I. Roy, T.Y. Ohulchanskyy, H.E. Pudavar, E.J. Bergey, A.R. Oseroff, J. Morgan, T.J. Dougherty, P.N. Prasad, Ceramic-based nanoparticles entrapping water-insoluble photosensitizing anticancer drugs: a novel drug-carrier system for photodynamic therapy, J. Am. Chem. Soc. 125 (2003) 7860–7865.
[30] J. Qian, A. Gharibi, S. He, Colloidal mesoporous silica nanoparticles with protoporphyrin IX encapsulated for photodynamic therapy, J. Biomed. Opt. 14 (2009) 014012.
[31] D. Brevet, M. Gary-Bobo, L. Raehm, S. Richeter, O. Hocine, K. Amro, B. Loock, P. Couleaud, C. Frochot, A. Morère, P. Maillard, M. Garcia, J.O. Durand, Mannose-targeted mesoporous silica nanoparticles for photodynamic therapy, Chem. Commun. 12 (2009) 1475–1477.
[32] T.Y. Ohulchanskyy, I. Roy, L.N. Goswami, Y. Chen, E.J. Bergey, R.K. Pandey, A.R. Oseroff, P.N. Prasad, Organically modified silica nanoparticles with covalently incorporated photosensitizer for photodynamic therapy of cancer, Nano Lett. 7 (2007) 2835–2842.
[33] G. Kantonis, M. Trikeriotis, D.F. Ghanotakis, Biocompatible protoporphyrin IX-containing nanohybrids with potential applications in photodynamic therapy, J. Photochem. Photobiol. A: Chem. 185 (2007) 62–66.
[34] K. Greish, Enhanced permeability and retention of macromolecular drugs in solid tumors: a royal gate for targeted anticancer nanomedicines, J. Drug Target. 15 (2007) 457–464.
[35] H. Maeda, G.Y. Bharate, J. Daruwalla, Polymeric drugs for efficient tumor-targeted drug delivery based on EPR-effect, Eur. J. Pharm. Biopharm. 71 (2009) 409–419.
[36] F. Venditti, R. Angelico, G. Palazzo, G. Colafemmina, A. Ceglie, F. Lopez, Preparation of nanosize silica in reverse micelles: ethanol produced during TEOS hydrolysis affects the microemulsion structure, Langmuir 23 (2007) 10063–10068.
[37] V. Simon, C. Devaux, A. Darmon, T. Donnet, E. Thiénot, M. Germain, J. Honnorat, A. Duval, A. Pottier, E. Borghi, L. Levy, J. Marill, Pp IX silica nanoparticles demonstrate differential interactions with *in vitro* tumor cell lines and *in vivo* mouse models of human cancers, Photochem. Photobiol. 86 (2010) 213–222.
[38] P. Roach, D. Farrar, C.C. Perry, Interpretation of protein adsorption: surface-induced conformational changes, J. Am. Chem. Soc. 127 (2005) 8168–8173.